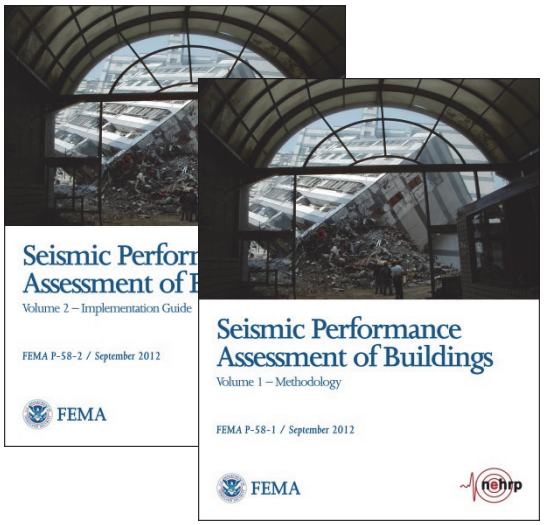

Background Document

FEMA P-58/BD-3.9.31

Acoustical Tile or Lay-in Panel Suspended Ceilings

Prepared by

Siavash Soroushian
Department of Civil and Environmental Engineering
University of Nevada, Reno
Reno, Nevada 89557

Submitted to

APPLIED TECHNOLOGY COUNCIL
201 Redwood Shores Parkway, Suite 240
Redwood City, California 94065
www.ATCouncil.org

Prepared for

FEDERAL EMERGENCY MANAGEMENT AGENCY
U.S. Department of Homeland Security
500 C Street, SW
Washington, D.C. 20472

September 2016

FEMA

nehrp

Background Documentation

FEMA P-58 Background Documents are a series of reports documenting the technical background and source information for key aspects of the FEMA P-58 methodology and its implementation. This report was developed over the course of the 5-year ATC-58-2 Project funded under FEMA Contract HSFE60-12-C-0243.

Background Documents were developed by consultants, serving at various levels within the project hierarchy, reporting the results of: (1) decisions on technical development protocols; (2) focused studies on the development of key aspects of the methodology; (3) documentation of recommended procedures; and (4) collection of available data for the development of structural and nonstructural fragilities. They were initially intended to serve as a record of the technical state-of-knowledge at the time they were produced, and as resources for the development of the eventual project reports. As such, they represent a snapshot in time, and may, or may not, match the technical content, recommended procedures, or data incorporated into the final methodology and its implementation.

This Background Document is intended for the purpose of providing supplemental knowledge to users of the FEMA P-58 methodology. Information contained herein has not been independently verified for accuracy as a stand-alone document, and may have been superseded in its final implementation within the methodology. Specifically in the case of certain nonstructural component fragilities, the NISTIR fragility classification numbering scheme was modified over the course of the project, and the fragility classification number assigned in this document might be different from numbers assigned in the final fragility database. Users of information in this document assume all liability arising from such use.

Notice

Any opinions, findings, conclusions, or recommendations expressed in this publication do not necessarily reflect the views of the Applied Technology Council (ATC), the Department of Homeland Security (DHS), or the Federal Emergency Management Agency (FEMA). Additionally, neither ATC, DHS, FEMA, nor any of their employees, makes any warranty, expressed or implied, nor assumes any legal liability or responsibility for the accuracy, completeness, or usefulness of any information, product, or process included in this publication. Users of information from this publication assume all liability arising from such use.

Cover photograph – Collapsed building viewed through the archway of an adjacent building, 1999 Chi-Chi, Taiwan earthquake (courtesy of Farzad Naeim, Farzad Naeim, Inc).

Development of Seismic Fragilities for Acoustical Tile or Lay-in Panel Suspended Ceilings for the ATC-58-2 Project

Siavash Soroushian

Structural Analyst | Advanced Technology & Research, Arup at San Francisco

Introduction

This document provides the basis for the seismic fragility values for acoustical tile or layin panel suspended ceilings (hereafter referred to as suspended ceilings) provided in the fragility spreadsheets for the ATC-58 project. Suspended ceilings are common in building construction and have been observed to be quite vulnerable during strong earthquake motions.

The history of suspended ceiling seismic research is summarized in Attachment 1 of this document which was prepared for the ATC-58 project by Keith Porter. It should be noted that while this previous research all provide valuable information, results from three major tests performed as part of a NSF research project called the Nonstructural NEES Grand Challenge project were used here. Several variables such as installation types, ceiling sizes, and direction of motions were considered in these experiments performed at the University of Buffalo (UB), University of Nevada, Reno and E-Defense shake table facilities. This document was prepared based on the reported observations from these experiment available in Ryu et al. (2015), Sorushian et al. (2015), and Jenkins (2015).

Because the experimental data from NSF Nonstructural Grand Challenge project did not cover all the ceiling installation types and suspended ceiling sizes, ATC-58 fragility values were developed based on limited judgment in combination with the available test data and observation. It is expected that future experimental and analytical projects will result in much more justifiable fragility values for ceiling systems.

Fragility Demand Parameter

According to previous research studies, it is well understood that suspended ceiling systems are sensitive to the acceleration motions of their supporting floor. It is likely that suspended ceiling systems are most sensitive to a narrow range of frequencies of input motion and amplitude of the vertical excitation. However, for purposes of ATC-58, the peak horizontal floor acceleration at the supporting (above) floor of suspended ceilings was selected as the demand parameter.

The testing data used to develop the fragility curves were obtained from the experiments performed as part of the Grand Challenge project. Specifically, tests performed at the University of Buffalo (UB) shake tables facility were used as the main source of establishing the fragility curves. During the UB experiments, the AC-156 Required Response Spectra (See Figure 1) was used as the target spectrum for the achieved motion at the ceiling support level. While some 1 and 2 directional testing was used during the experiments, most of the suspended ceiling specimens were tested under 3 directional motions. In addition to the UB

experiments, few test results performed at University of Nevada, Reno and E-Defense shake table facilities were used to perform a comparison with the developed fragility data. The direct measurement of peak supporting floor (frame) acceleration during the experiments was used as the Peak Floor Acceleration (PFA) demand parameter.

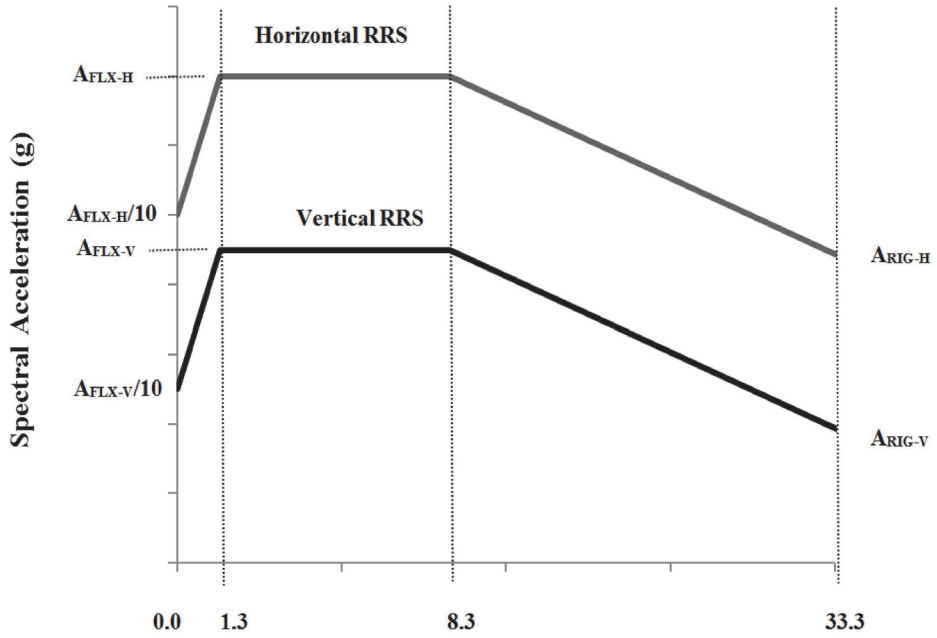

Figure 1. Required Test Response Spectra of AC-156 (5 % damped)

Damage States and Consequences

For purposes of the ATC-58 project, the following 3 damage states were adopted for the fragility spreadsheets.

Damage State 1, DS1 – 5% of ceiling grid and tile damage – Consequence: reinstall, repair, or replace 5% of the ceiling area

Damage State 2, DS2 – 30% of ceiling grid and tile damage – Consequence: replace 30% of the ceiling area

Damage State 3, DS3 – 50% of ceiling grid and tile damage – Consequence: replace the whole ceiling

Currently, several fragility values and curves are available for suspended ceilings. While all of these studies provided valuable information, not a consistent approach was used to obtain fragility parameters for the suspended ceilings. As an example, not a single damage states were previously assigned to a suspended ceilings with 40% unseated perimeter members. Therefore, a unified approach is needed to assign certain damage state to a ceiling condition with less dependency on the inspector judgment.
In order to find the percentage of fallen area, a determination process (as shown in Table 1) was used to equate the damage observed to an amount of fallen panels. As shown in this table, in addition to the number of fallen ceiling panels, equivalent number of failed panels is

considered for different types of grid (connection) damage based on the affected ceiling area and needed repair effort.

Table 1. Percentage of equivalent fallen ceiling area determination process

Damage Type	Description	Equivalent Number of Failed Panels
Perimeter Damage	Pop rivet failure	2
	Seismic clip failure or crushing	2
	Unseating of grid members from wall angle	2
Grid Damage	2 ft. grid member joint damage, buckling	2
	4 ft. grid member joint damage, buckling	4
	Main Run joint damage, buckling	Up to 48
Tile Damage	Fallen panels	1
	Misaligned tiles	0

Ceiling Installation Types

For purposes of the ATC-58 project, two basic installation types were adopted for the fragility spreadsheets. These are no seismic bracing and detailing (typically found in Seismic Design Categories A, B and exempt area of other Seismic Design Categories) and seismically braced and detailed in accordance Seismic Design Category D, E and F requirements of ASCE 7-05 and ASTM E-580. Seismic Design Category C and requirements are between those of A, B and D, E. Since Grand Challenge Testing Data for C configurations, they have been assumed to be the same as A,B.

Specific Details of Seismically Unbraced Configuration (SDC A, B and C)

Perimeter Ledge Angle = 7/8 inch wide

Grid Duty = Intermediate

Diagonal Splay Wire Bracing = none

Compression Posts = none

Tile Weight = less than 2 psf

Attached perimeter = none

Specific Details of Seismically Braced Configuration (SDC D, E and F)

Perimeter Ledge Angle = 2 inch wide

Grid Duty = Heavy

Diagonal Splay Wire Bracing = yes

Compression Posts = yes

Tile weight = less than 2 psf

Attached perimeter = two (adjacent sides)

In addition it is assumed that that for Suspended Ceilings assigned SDC F, the ceiling system will be designed to higher design requirements and installed with rigorous Q/A and inspection.

Ceiling Installation Areas

Ceiling seismic codes and standards have provided increased seismic requirements based on ceiling area with greater detailing being required for larger ceiling areas. The ceiling areas with these ceiling requirements change are 144 square feet, 1000 square feet and 2500 square feet.

For purposes of the ATC-58 project, the following ceiling installation areas have been adopted for fragilities provided in the spreadsheets:

Ceiling Area

a) Less than 250 square feet
b) 250 – 1000 square feet
c) 1000 – 2500 square feet
d) Greater than 2500 square feet

Separate fragility values are developed for spreadsheets for each area. The 250 square foot area was adopted because of desires to not have normative quantities in any smaller units.

In order to consider the effect of suspended ceiling sizes, it was assumed that the acceleration demand that causes the major damage state ceiling is related to the tributary seismic force in the direction of motion at the intersection of the ceiling grid to the perimeter ledger angle. It was also assumed that tributary area is directly proportional to the length, L of the ceiling in the direction of motion. In the biaxial (2D) or triaxial (3D) tests, L was considered as the length of the longer side of the rectangular-shape suspended ceilings.

For purposes of establishing fragilities for these areas, it is assumed that the ceilings are square in plan. For square areas, the tributary length L = square root of the Ceiling Area. Since the ceiling areas are for a range of values, it was necessary in establishing the fragility values to assume a specific area for each range. The following are the values assumed and the resulting tributary length:

Ceiling Area	Area	Assumed L (feet)
e) Less than 250 square feet	250	16
f) 250 – 1000 square feet	625	25
g) 1000 – 2500 square feet	1764	42
h) Greater than 2500 square feet	2500	50

Fragility Value Determination Procedure

As mentioned earlier, the testing data from a series of tests performed at the UB, UNR, and E-Defense shake table studies were used to assess the suspended ceiling fragility parameters. Table 1, Table 2, and Table 4 shows the suspended ceiling assemblies considered here from these test series. Throughout this report, unbraced ceiling data are highlighted in the tables.

Table 2. UB test matrix

Assembly #	Size (Nominal) (ft^2)	Input Direction	Grid Duty	Panel Weight (psf)	Lateral restraints	Perimeter Angle (in.)	Plenum Height (in.)
Performed on 20ft. × 50ft. test frame							
3	20×50	*x*	Heavy	1.05	Yes	2	29
4	20×50	3D	Heavy	1.05	Yes	2	29
7	20×50	3D	Heavy	1.05	No	7/8+clip	29
8	20×50	3D	Interm-ediate	1.05	No	7/8	29
Performed on 20ft. × 20ft. test frame							
11	20×20	3D	Heavy	1.05	No	7/8+clip	29
12	20×20	3D	Heavy	1.05	Yes	2	29
13	16×16	3D	Heavy	1.05	No	7/8+clip	29
14	16×16	3D	Heavy	1.05	Yes	2	29

*The description of those tests discussed here is presented

Table 3. UNR test matrix

Assembly #	Size (Nominal) (ft^2)	Input Direction	Grid Duty	Panel Weight (psf)	Bracing	Perimeter Angle (in.)	Plenum Height (in.)
2	58 X 10	1D	Heavy	1.31	Yes	2	36
17	28 X 10	1D	Heavy	1.31	Yes	2	36
20	58 X 10	1D	Heavy	1.31	Yes	2	36

*The description of those tests discussed here is presented

Table 4. E-Defense test matrix

Floor #	Size (Nominal) (ft^2)	Input Direction	Grid Duty	Panel Weight (psf)	Bracing	Perimeter Angle (in.)	Plenum Height (in.)
4	33×40	3D-2D	Heavy	0.72	No	7/8+clip	36
5	33×40	3D-2D	Heavy	0.72	Yes	7/8+clip	36

The equivalent percentage of damaged suspended ceiling area with respect to the PFA were determined based on the reports available for each run of the above experiments. An example of such an evaluation is presented in **Error! Reference source not found.** for the Assembly #4 at UB experiment. It should be noted that the test results of the braced ceiling at E-Defense experiment was not considered because of the early damage in the ceiling due to (mainly) excessive vertical excitation. The summary of equivalent percentage of damaged ceiling area is presented in Table 5.

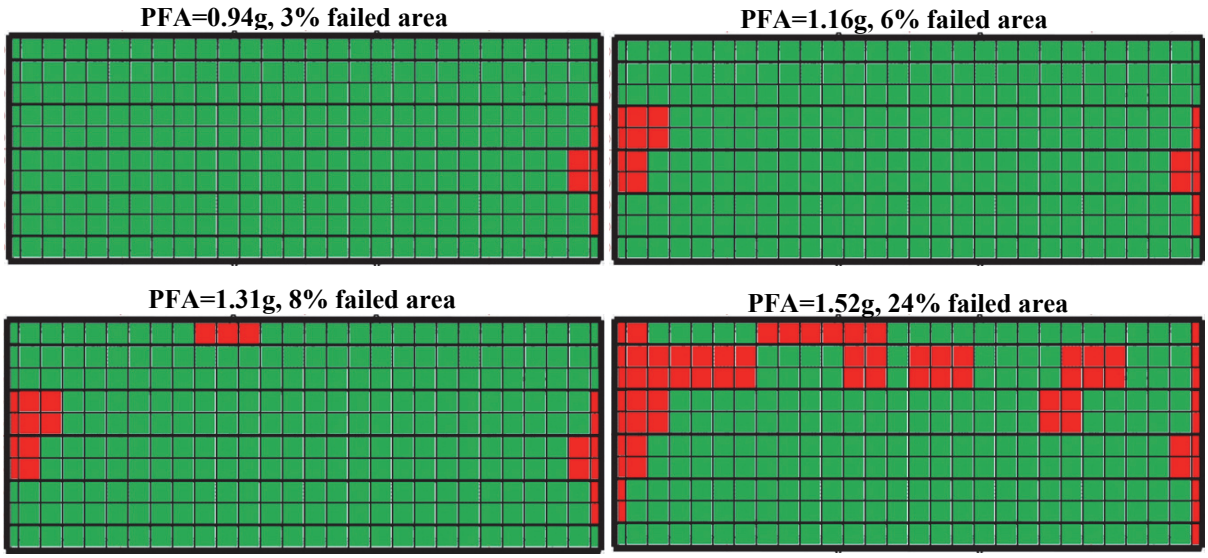

Figure 2 Propagation of the damage at UB experiment, assembly #4

Table 5. Ratio of failed ceiling area and associated PFA (g)

UB Experiment							
Assembly #3	PFA	0.72	0.91	1.03	1.31	1.49	
	Failed Area	0.02	0.03	0.03	0.05	0.81	
Assembly #4	PFA	0.94	1.16	1.31	1.52		
	Failed Area	0.03	0.06	0.08	0.24		
Assembly #7	PFA	0.72	0.91	1.03	1.31	1.49	
	Failed Area	0.007	0.014	0.03	0.08	0.42	
Assembly #8	PFA	0.42	0.58	0.76	0.87	1.12	1.24
	Failed Area	0.03	0.05	0.09	0.15	0.26	0.68
Assembly #11	PFA	1.54	1.81	2.1			
	Failed Area	0.17	0.24	0.73			
Assembly #12	PFA	1.76	2.02	2.33			
	Failed Area	0.14	0.42	0.63			
Assembly #13	PFA	1.99	2.25	2.52			
	Failed Area	0.13	0.52	0.86			
Assembly #14	PFA	1.65	1.95	2.28			
	Failed Area	0.06	0.52	0.84			
UNR Experiment							
Assembly #2	PFA	1.24	1.27				
	Failed Area	0.04	0.06				
Assembly #20	PFA	1.21					
	Failed Area	0.05					

A power-law regression analysis of the failed suspended ceiling area and PFA was used to develop continues demand model and estimate the demand parameters in equation (1) and equation (2) (Cornell et al. 2002):

$$S_d = a(PFA)^b \tag{1}$$

$$\beta_d = \sqrt{\frac{\sum_{i=1}^{N}\left(\ln ratio_i - ln(a(PFA)^b)\right)^2}{N-2}} \tag{2}$$

where S_d is the median of the demand estimate, a and b are unknown regression coefficients, $ratio_i$ is the ratio of failed suspended ceiling area corresponding to the i^{th} motion, and N is the total number of data points. Also, undamaged suspended ceiling conditions with their corresponding PFA were represented with a line with the constant value (ratio) of 0.001. An example of this regression process is presented in Figure 3. Summary of regression parameters for all UB assemblies are presented in Table 6.

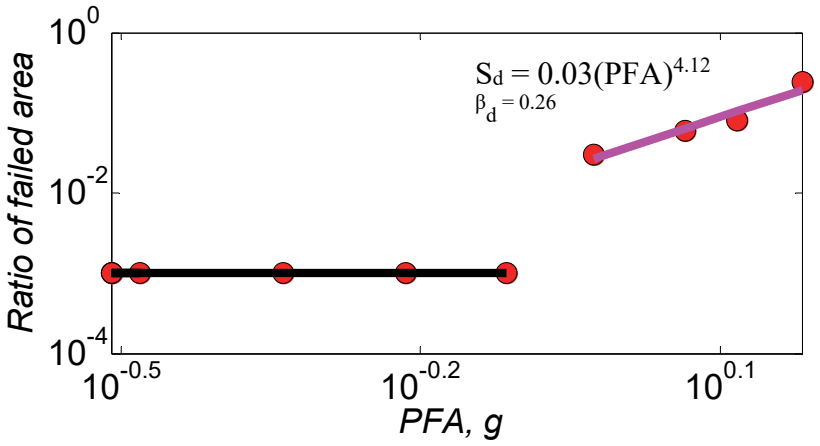

Figure 3. Demand model for the assembly #4 at UB experiment

The segmental fragility curves were then developed for UB ceiling assemblies based on the damage states defined earlier and demand parameters presented in the Table 6 by using equation **Error! Reference source not found.** (Nielson and DesRoches, 2007):

$$P[D > C|PFA] = \Phi\left(\frac{\ln\left(\frac{S_d}{S_c}\right)}{\beta_d}\right) \tag{3}$$

where S_d is the median seismic demand estimate, S_c is the median estimate of the damage state capacity, β_d is the logarithmic standard deviation of the demand estimate, and $\Phi[\cdot]$ is the standard normal cumulative distribution function.

By using the least square approach between equation (3) and two segmental fragility curves, the best single combined fragility curve were obtained. The median and dispersion values obtained from this fitting approach is denoted as θ and β_r, respectively. Due to the uncertainty in the adequate number of test data and experimental condition, uncertainty dispersion $\beta_u = 0.25$ was considered here. Therefore the total dispersion (β) for the fragility curves was considered as:

$$\beta = \sqrt{\beta_u^2 + \beta_r^2} \tag{4}$$

An example of such a calculation process is presented in Figure 4. The median θ and dispersion of fragility curves calculated for the UB experiments are presented in Table 7.

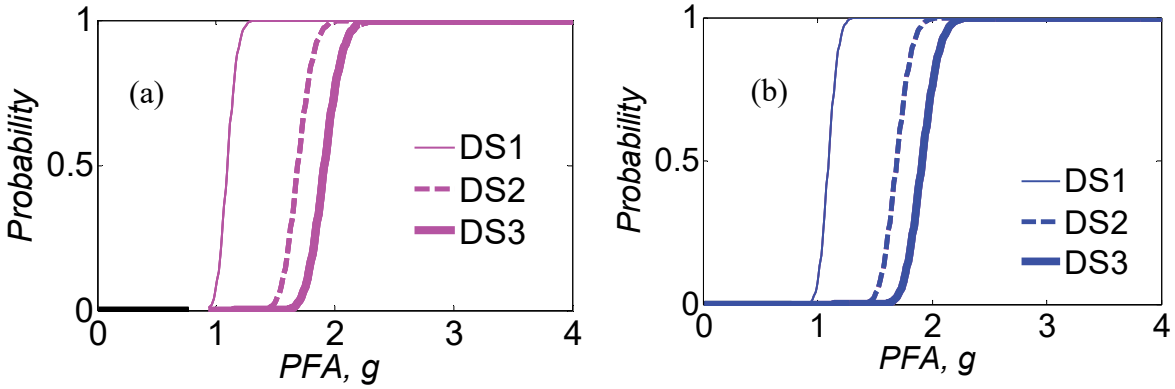

Figure 4. Fragility curves for the assembly #4 at UB experiment; (a) segmental curves; (b) combined curves

Table 6. Regression parameters of the damaged suspended ceilings

UB Experiment			
	a	**b**	β_d
Assembly #3	0.005	5.32	1.00
Assembly #4	0.03	4.12	0.26
Assembly #7	0.03	5.35	0.47
Assembly #8	0.24	2.69	0.32
Assembly #11	0.019	4.66	0.34
Assembly #12	0.008	5.35	0.29
Assembly #13	0.0005	8.05	0.33
Assembly #14	0.001	8.21	0.65

Table 7. Medians and Dispersion of Fragility Curves

UB Experiment						
	DS1		**DS2**		**DS3**	
	θ	**β**	**θ**	**β**	**θ**	**β**
Assembly #3	1.56	0.31	2.18	0.31	2.40	0.31
Assembly #4	1.09	0.26	1.69	0.26	1.91	0.26
Assembly #7	1.10	0.27	1.54	0.27	1.70	0.27
Assembly #8	0.56	0.28	1.08	0.28	1.31	0.28
Assembly #11	1.43	0.25	1.79	0.26	2.00	0.26
Assembly #12	1.64	0.25	1.98	0.25	2.18	0.25
Assembly #13	1.86	0.25	2.17	0.25	2.32	0.25
Assembly #14	1.60	0.26	1.95	0.26	2.07	0.26

UB suspended ceiling assemblies #4, #12, and #14 were tested under triaxial excitations and have had same installation type as defined previously for the seismically braced suspended ceilings. By using linear regression analysis between the median of fragility values versus the tributary length (L), the fragility values for different sizes (areas) of the seismically braced ceilings were obtained. Such a regression curves along with their equations are presented in Figure 5.

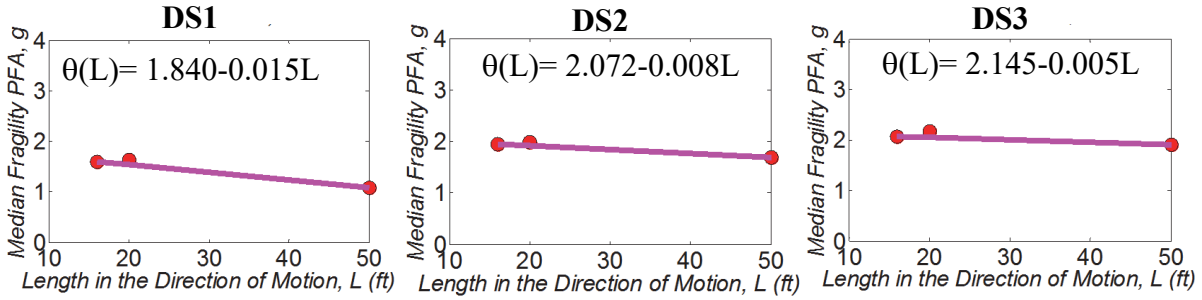

Figure 5. Estimate on the effect of braced ceiling sizes on the median of fragility curves

It should be mentioned that the above equations are approximation and may not be accurate for several situation. As an example, by comparing to UB test assemblies #3 and #4, it can be found the motion directivity (1D versus 3D) can result in up to 30% difference. Such an effect is presented in Figure 6.

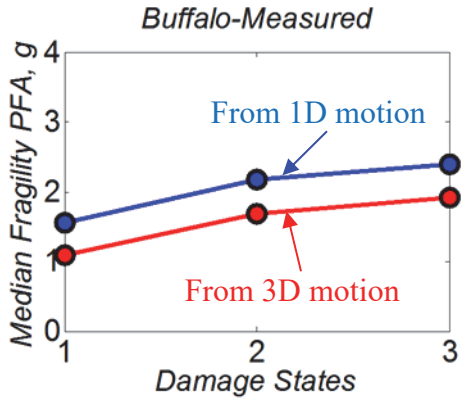

$DS1_{3D} \approx 0.7\ DS1_{1D}$

$DS2_{3D} \approx 0.8\ DS2_{1D}$

$DS3_{3D} \approx 0.8\ DS3_{1D}$

Figure 6. Effect of motion directivity on the median fragility values of braced suspended ceilings

The PFA value that corresponds to DS1 (5% damaged area) based on the equation presented in Figure 5 and for the larger size of the suspended ceiling at the UNR (L=58ft) is 1.35g, including the effect of motion directivity. According to the UNR experiment, the PGAs that caused 5% damaged area were around 1.25g, which is in close range of the value estimated by the regression analysis.

The fragility parameters of seismically braced configuration (SDC D and E) for all suspended ceiling sizes are obtained (see Table 8) from the equations presented in Figure 5, assuming acceptable accuracy. It was also further assumed based on the judgment that these values are increased by 20% for seismically braced configuration (SDC F) (see Table 9). It should be noted that the maximum dispersion value of braced ceiling, based on UB experiment (0.26 from Table 7), is rounded up to 0.30 in this table.

Table 8. Medians and Dispersion of Fragility Curves for suspended ceiling with Seismic Design Categories D and E (SDC D, E) (Ip =1.0)

Seismic Design Categories D and E (SDC D, E) (Ip =1.0)

	A < 250ft C3032.003a		**250ft<A<1000 C3032.003b**		**1000ft<A<2500 C3032.003c**		**A > 2500ft C3032.003d**	
	θ	**β**	**θ**	**β**	**θ**	**β**	**θ**	**β**
DS1	1.60	0.30	1.47	0.30	1.21	0.30	1.09	0.30
DS2	1.95	0.30	1.88	0.30	1.75	0.30	1.69	0.30
DS3	2.07	0.30	2.03	0.30	1.95	0.30	1.91	0.30

Table 9. Medians and Dispersion of Fragility Curves for suspended ceiling with Seismic Design Categories F (SDC F) (Ip =1.5)

Seismic Design Categories D through F (SDC D, E, F) (Ip =1.5)

	A < 250ft C3032.004a		**250ft<A<1000 C3032.004b**		**1000ft<A<2500 C3032.004c**		**A > 2500ft C3032.004d**	
	θ	**β**	**θ**	**β**	**θ**	**β**	**θ**	**β**
DS1	1.92	0.30	1.76	0.30	1.45	0.30	1.31	0.30
DS2	2.34	0.30	2.26	0.30	2.10	0.30	2.03	0.30
DS3	2.48	0.30	2.44	0.30	2.34	0.30	2.29	0.30

UB assembly #8 was the only tested suspended ceiling that had same installation type as the definition of the unbraced suspended ceilings that was given earlier. Therefore, UB assemblies #7, #11, and #13 that have slightly different installation types, but still unbraced ceiling, were used to study the trend (slope) of median fragility variations with respect to the suspended ceiling tributary length (L). The curve of the linear regression analysis for the later three suspended ceilings is presented in Figure 7. To examine such a trend, the damage observation of unbraced suspended ceiling system from E-Defense experiment was used, which had similar installation detail with the mentioned three subassemblies. According to this linearization and L value of 40ft for the E-Defense test, the PFA corresponding to DS1 (5% damaged are) is estimated to be 1.26. From the E-Defense observation, only few (up to three) panels were failed under the maximum PFA of 1.19g, which is less than the 1.26g estimated by the regression analysis.

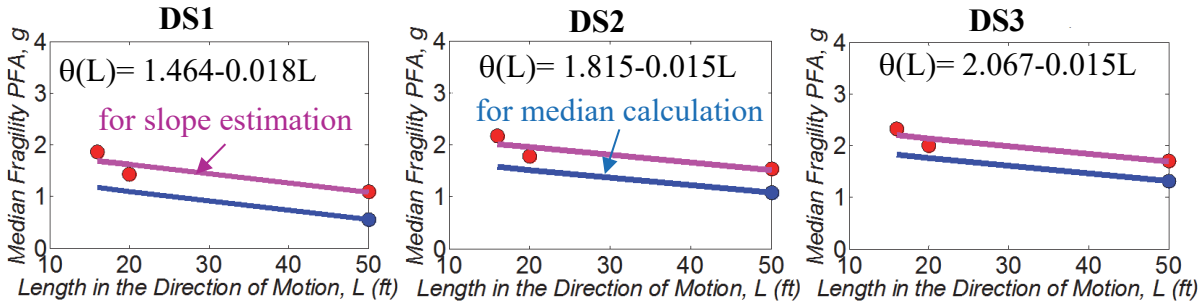

Figure 7. Estimate on the effect of unbraced ceiling sizes on the median of fragility curves

The fragility parameters of unbraced configuration (SDC A, B and C) for all suspended ceiling sizes are calculated (see Table 10) from the equations (presented in Figure 7) obtained by the slope of the lines from the regression analysis passing through the UB assembly #8 fragility values. It should be noted that the maximum dispersion value of unbraced ceiling, based on UB experiment (0.28 from Table 7), is rounded up to 0.30 in this table.

Table 10. Medians and Dispersion of Fragility Curves for suspended ceiling with Seismic Design Categories A through C (SDC A, B and C)

	Seismic Design Categories A through C (SDC A, B and C)							
	A < 250ft C3032.001-2a		**250ft<A<1000 C3032.001-2b**		**1000ft<A<2500 C3032.001-2c**		**A > 2500ft C3032.001-2d**	
	θ	**β**	**θ**	**β**	**θ**	**β**	**θ**	**β**
DS1	1.17	0.30	1.01	0.30	0.70	0.30	0.56	0.30
DS2	1.58	0.30	1.45	0.30	1.20	0.30	1.08	0.30
DS3	1.82	0.30	1.69	0.30	1.43	0.30	1.31	0.30

Conclusions

The resulting fragility values and dispersions used in the fragility spreadsheets for the ATC-58 project based on the above procedure are provided in Table 11 of this document.
It is recognized that the values provided are based up a great many unsubstantiated assumptions, extrapolations and judgments. It is expected that future experimental and

analytical projects will result in much improved and substantiated fragility values for ceiling systems.

Table 11. Medians and Dispersion of Fragility Curves for suspended ceilings

Seismic Design Categories A through C (SDC A, B and C)

	A < 250ft C3032.001-2a		250ft<A<1000 C3032.001-2b		1000ft<A<2500 C3032.001-2c		A > 2500ft C3032.001-2d	
	θ	β	θ	β	θ	β	θ	β
DS1	1.17	0.30	1.01	0.30	0.70	0.30	0.56	0.30
DS2	1.58	0.30	1.45	0.30	1.20	0.30	1.08	0.30
DS3	1.82	0.30	1.69	0.30	1.43	0.30	1.31	0.30

Seismic Design Categories D and E (SDC D, E) (Ip =1.0)

	A < 250ft C3032.003a		250ft<A<1000 C3032.003b		1000ft<A<2500 C3032.003c		A > 2500ft C3032.003d	
	θ	β	θ	β	θ	β	θ	β
DS1	1.60	0.30	1.47	0.30	1.21	0.30	1.09	0.30
DS2	1.95	0.30	1.88	0.30	1.75	0.30	1.69	0.30
DS3	2.07	0.30	2.03	0.30	1.95	0.30	1.91	0.30

Seismic Design Categories D through F (SDC D, E, F) (Ip =1.5)

	A < 250ft C3032.004a		250ft<A<1000 C3032.004b		1000ft<A<2500 C3032.004c		A > 2500ft C3032.004d	
	θ	β	θ	β	θ	β	θ	β
DS1	1.92	0.30	1.76	0.30	1.45	0.30	1.31	0.30
DS2	2.34	0.30	2.26	0.30	2.10	0.30	2.03	0.30
DS3	2.48	0.30	2.44	0.30	2.34	0.30	2.29	0.30

References

Cornell, A. C., Jalayer, F., Hamburger, R. O., and Foutch, D. A., 2002. Probabilistic basis for 2000 SAC federal emergency management agency steel moment frame guidelines." J. Struct. Eng, 10.1061/ (ASCE) 0733-9445(2002)128:4(526), 526–533.

Jenkins, C., 2015. *Experimental Seismic Evaluation of Ceiling-Piping-Partition Nonstructural Systems,* Master Thesis, Dept. of Civil and Environmental Engineering, Univ. of Nevada, Reno, NV.

Ryu, K.P., Reinhorn, A.M., and Filiatrault, A., 2015. *Capacity Evaluation of Suspended Ceiling System*. Technical Report MCEER-15-XXXX, Buffalo, NY. (in review).

Soroushian, S., Maragakis, M., Ryan, K., Sato, E., Sasaki, T., Okazaki, T., and Mosqueda, G., 2015. *Seismic Simulation of Integrated Ceiling-Partition Wall-Piping System at E-*

Defense, Part 2: Evaluation of Nonstructural Damage and Fragilities, Journal of Structural Engineering, ASCE, In Press.

Nielson, G. B., and DesRoches, R., 2007. *Analytical seismic fragility curves for typical bridges in the central and southeastern United States*. Earthquake Spectra, 23(3), 615–633.

ATTACHMENT 1- LITERATURE REVIEW OF CEILING RESEARCH

ANCO Engineers, Inc., (1983) performed full-scale shake-table tests on a light acoustical tile ceiling system. A variety of lateral restraint systems were tested, and the ceiling was subjected to a variety of shaking regimens. The report discusses ceiling performance under each test, providing peak diaphragm acceleration, peak ceiling acceleration, and horizontal peak response spectrum ordinate of actual table motion. Two tests produced incipient ceiling failure at 0.8g and 1.0g; the ceiling was tested to collapse in one test, at a peak diaphragm acceleration of 2.0g.

Rihal and Granneman (1984) present results of 12 full-scale dynamic tests of suspended ceilings under a variety of installation conditions. All tests are of a ceiling system 12 ft. x 16 ft. in plan, with 2 ft. x 4 ft. exposed grid elements and lay-in acoustical tiles. The authors find that the behavior of ceilings is influenced by input acceleration and frequency. They find that ceiling perimeter details significantly influence damage, and note that the presence of hangers near the ends of grid elements mitigates drop-out of ceiling tiles at the perimeter.

Griffin and Tong (1992) report observations of ceiling performance in more than 100 electric power and industrial facilities affected by the Loma Prieta and Whittier earthquakes. The authors present three major conclusions. First, ceiling damage was widespread, with more than half of these facilities experiencing some damage to suspended ceilings. Second, there is no obvious threshold of peak ground acceleration causing ceiling damage, with some damage occurring at PGA values below 0.10g, and some facilities experiencing no ceiling damage despite PGA in excess of 0.50g. Finally, all observed ceiling damage is attributable to tensile failure of grid connections, compression failure of grid elements, falling of above-ceiling components, and interaction of the ceiling with overhead utilities. The authors also note that perimeter connection of the grid to the wall acts as the de facto seismic restraint of the ceiling; diagonal bracing do not become active.

Eidinger and Goettel (1998) offer, without supporting evidence or a clear definition of damage states, fragility functions for suspended ceilings as a function of peak ground acceleration (not peak diaphragm acceleration). For the slight and complete damage states, which might correspond best to the DS1 and DS2 of interest here, they recommend PGA capacity values of 0.5g and 1.3g, respectively, with $\beta = 0.5$ and 0.4, respectively. Considering the commonly used zero-period acceleration amplification of 1.0 for the bottom 1/3rd of a building, 1.5 for the middle 1/3rd, and 2 for the top 1/3rd of a building, these median values might reasonably correspond to $x_m = 0.8$g and 2.0g in terms of peak diaphragm acceleration. Note however that they accompany their recommended capacity for DS2 with the note, "add compression struts," suggesting that these capacities are for a ceiling system without compression struts.

Porter (2000). As part of a doctoral thesis, the present author proposed an analytical methodology to estimate the fragility of suspended ceilings. It considered six possible failure modes (e.g., buckling of grid members, shearing of pop rivets, etc.), accounted for uncertainty in a number of variables, and made the median capacity a function of ceiling dimensions. Only a single ceiling system was considered, with 2x4 ceiling tiles (same unit weight as those considered here) and lay-in light fixtures of a particular weight and spacing. Monte Carlo simulation was used to generate samples of eight uncertain variables and to calculate six performance functions (one for each failure mode) and to determine collapse

capacity as a function of ceiling dimensions (length and width) and peak diaphragm acceleration. It was found that the logarithmic standard deviation of collapse capacity was fairly constant ($\beta = 0.8$), and a curve was fit to the median capacity x_m, as a function of length + width. The model was compared with the empirical studies, which suggested that the model produced reasonable results.

Badillo-Almaraz et al. (2006) performed full-scale laboratory tests of 16x16-ft suspended ceilings specimens with sway braces at the ceiling's single compression strut, and six different configurations: (1) undersized tiles (i.e., tiles slightly smaller than their nominal dimensions), (2) undersized tiles with retainer clips, (3) undersized tiles with recycled grid components, (4) normal sized tiles, (5) normal sized tiles with retainer clips and (6) normal sized tiles without the (single) compression post. The test simulated wall capture all around, i.e., the ceiling perimeter support was not free to move relative to the frame. All ceilings had 2x2-ft tiles (4 times the size of the ceiling considered here), no lay-in light fixtures (which occur in the ATC-58 ceiling), and tiles with mass of either 0.94 psf or 0.72 psf (significantly lighter than the tiles considered here). Each specimen was subjected to a sequence of 33 excitation histories, including unidirectional and bidirectional (longitudinal and vertical) white-noise excitations, as well as unidirectional and bidirectional earthquake excitations with varying degrees of short-period spectral accelerations from 0.25g to 2.5g in 0.25-g increments. They created fragility functions for four damage states: (DS1) 1% of tiles fall; (DS2) 10% of tiles fall; (DS3) 33% of tiles fall; and (DS4) Part or all of grid collapses (meaning cross-tees are bent or fall or otherwise must be replaced).
The authors created empirical fragility functions for these damage states in terms of the 5%-damped spectral acceleration of the floor below the ceiling, not above, at periods ranging from 0 sec to 2.0 sec in 0.5-sec increments, but based on the observed transfer function from base of the frame (the slab below the ceiling) to the top of the frame (akin to the slab above), the amplification at periods of interest (around 0.7 Hz for a mass suspended the same length as the wire), the amplification is perhaps 1.1x.
Configurations 4 or 6 might be most relevant here. Considering peak floor below acceleration (PFA) as the EDP, the fragility functions for configuration 4, DS1, DS2, DS3, and DS4 produced for this configuration had median capacities in terms of PFA equal to 1.1, 1.4, 2.0, and 1.7g, respectively, or approximately $x_m = 1.2$, 1.5, 2.2, and 1.9g respectively for peak diaphragm acceleration for the floor above (PDA). The estimated logarithmic standard deviations were $\beta = 0.12$, 0.20, 0.14, and 0.11, respectively, which are probably low because of uniformity in design, construction, and excitation. Failure appeared primarily to be initiated by buckling of grid members and pop-rivet shear failure. Capacities for configuration 6 are almost identical, suggesting that the presence of a single compression post (on one grid member each way) made little difference to collapse.

REFERENCES CITED IN LITERATURE REVIEW

ANCO Engineers, Inc., 1983. *Seismic Hazard Assessment of Nonstructural Ceiling Components – Phase I*, National Science Foundation grant CEE-8114155, Culver City, CA.

Badillo-Almaraz, H., A.S. Whittaker, A.M. Reinhorn, and G.P. Cimellaro, 2006. *Seismic Fragility of Suspended Ceiling Systems*, Technical Report MCEER-06-0001, Multidisciplinary Center for Earthquake Engineering Research, Buffalo, NY, 225 pp.

Eidinger, J., and K. Goettel, 1998. Benefits and costs of seismic retrofits of non structural components of hospitals, essential facilities, and schools. *Proc., Seminar on Seismic Design Retrofit and Performance of Nonstructural Components, ATC 29-1,* Applied Technology Council, Redwood City, CA, 491-504.

Griffin, M.J., and W. Tong, 1992. Performance of suspended ceilings in earthquakes with recommended strengthening techniques for damage mitigation. *ATC-29: Proc., Seminar and Workshop on Seismic Design and Performance of Equipment and Nonstructural Elements in Buildings and Industrial Structures; Irvine, California, October 3-5, 1990,* Applied Technology Council, Redwood City, CA pp. 75-85.

Porter, K.A., 2000. *Assembly-Based Vulnerability of Buildings and its Uses in Seismic Performance Evaluation and Risk-Management Decision-Making.* Doctoral Dissertation, Stanford University, Stanford, CA, and ProQuest Co., Ann Arbor, MI, pub. 99-95274, 196 pp.

Rihal, S.S., and G. Granneman. 1984. Experimental investigation of the dynamic behavior of building partitions and suspended ceilings during earthquakes. *Proceedings of the Eighth World Conference on Earthquake Engineering, July 21-28, 1984, San Francisco*, Englewood Cliffs, NJ: Prentice-Hall, pp.1135-1142.